Pre-administration of a carboxypeptidase inhibitor enhances plasminogen accumulation and thrombolysis after tPA infusion: Demonstration by real-time intravital imaging analysis of microthrombi in mice

Pre-administration of a carboxypeptidase inhibitor enhances plasminogen accumulation and thrombolysis after tPA infusion: Demonstration by real-time intravital imaging analysis of microthrombi in mice

Dissertation by:

Nitty Skariah Mathews

Course: Cooperative Major in Medical Photonics

Department of Medical Physiology

Hamamatsu University School of Medicine

List of Abbreviations and Acronyms

rt-PA	recombinant tissue-type plasminogen activator
FDA	Food and Drug Administration
Glu-plg	Glu-plasminogen
TPE	two-photon excitation
NA	numerical aperture
PSF	point spread function
TF	tissue factor
DVT	deep vein thrombosis
LBS	lysine-binding site
CTL	carboxy-terminal lysine
tPA	tissue-type plasminogen activator
TAFI	thrombin-activatable fibrinolysis inhibitor
TAFIa	activated thrombin-activatable fibrinolysis inhibitor
TM	thrombomodulin
PTCI	carboxypeptidase inhibitor from potato tuber
EACA	epsilon aminocaproic acid
ROI	region of interest
RFI	relative fluorescence intensity
AF555	Alexa Fluor 555

INTRODUCTION

Background:

The WHO Global Health Estimates 2019 show that cardiovascular diseases account for over 30% of all global deaths, the major contributors being ischemic heart diseases including myocardial infarction and ischemic stroke.[1] In these conditions, unyielding thrombi occlude vital blood vessels, and timely thrombolysis using pharmacological agents or endovascular thrombectomy is warranted. Recombinant tissue-type plasminogen activator (rt-PA) has been the pharmacological agent of choice since its approval by FDA for these conditions. However, this drug has been widely underutilized due to a narrow therapeutic window or other pre-existing risk factors. In those patients who do receive thrombolytic therapy, around 11% endure bleeding incidents, and approximately 2% of them suffer a severe bleeding event such as a symptomatic intracranial hemorrhage.[2,3] Despite these shortcomings, not much progress has been made over the years to overcome these limitations. However, thanks to the advances in imaging technology and molecular sciences in recent years, there is a deeper understanding of the pathophysiological mechanisms underlying thrombosis and fibrinolysis. This gives hope for better diagnostic and therapeutic strategies targeting thrombotic diseases.

Imaging in life science research

Modern imaging technologies and digital image processing techniques permit visualization of protein dynamics and other complex biological pathways at the cellular and subcellular level in real-time. Previously, these were limited by the diffraction limit of light which is the maximum attainable spatial resolution by conventional microscopy.[4] The intensity distribution

of the image of a very small sample/ object is called the point spread function (PSF).[5] The resolving power or resolution of a microscope is the ability to visualize two adjacent points as distinct entities. The Rayleigh criterion specifies the minimum distance between two light sources that can be resolved into two separate objects[6] while the numerical aperture (NA) of a microscope objective is a measure of its ability to gather light and resolve fine specimen detail at a fixed object distance. The resolution of an optical system depends on the NA of the objective used. The higher the NA of the objective, the higher the resolution attained.[7] Improving the resolving power of a microscope beyond the diffraction limit of light (200 nm) had been a problem that challenged researchers for several years. As a result of innovations in optics and technology, the last 3-4 decades have seen numerous developments in the field of microscopy. Most of the knowledge regarding biological phenomena at the cellular and subcellular level has been generated by visualizing them directly. Among the available techniques, fluorescence microscopy is the most widely used for this purpose. It allows cellular components to be observed by specific protein labeling and real-time imaging of structures inside a living sample. However, diffraction of light limits the spatial resolution achievable by conventional fluorescence microscopy.

One of the most well-established and widely used microscopy techniques is the confocal microscope first described by Marvin Minsky in 1955.[8] This technique uses point illumination via a pinhole to eliminate out-of-focus light in image formation. Modern confocal microscopes incorporate advances in optics and electronics and improve the speed of image generation and image quality. Today, lasers are the most commonly used light source for complex fluorescence microscopy techniques and in combination with a confocal optical system, it is called confocal laser scanning microscopy. However, photobleaching of fluorescent probes and phototoxicity are drawbacks seen with confocal fluorescence microscopy.[9]

Two-photon excitation microscopy

In recent times, non-linear microscopy techniques such as two-photon excitation (TPE) microscopy and second harmonic generation are increasingly used. They improve the PSF and try to achieve a higher image resolution. In these methods, the rate at which the photon excitation occurs depends nonlinearly on the intensity. Maria Göppert-Mayer first described theoretically in 1931 the coaction of two photons that together produce an excitation energy that is the sum of that of the individual photons.[10] It was however first demonstrated and popularized five decades later by Denk and colleagues[11] after the invention of lasers.

In TPE microscopy, a pulsed laser is used such that two photons near-simultaneously interact with a molecule at femtosecond intervals to generate enough excitation fluorescence for imaging. Each of these photons has half the energy as the corresponding single photon. As the energy of a photon is inversely proportional to its wavelength, in TPE, the wavelength of the photons should be approximately twice as much as required for one-photon excitation. For example, if a fluorophore absorbs light at 450 nm under single-photon excitation, the corresponding TPE would require a wavelength of ~900 nm. Thus, TPE can be excited by infra-red illumination rather than ultra-violet-visible wavelength illumination. For two photons to be simultaneously absorbed, significantly higher laser power is required compared to conventional one-photon excitation. A pulsed laser source with peak power in each pulse is used for this purpose. These days, a mode-locked titanium sapphire (Ti:S) laser is most commonly used. Commercial Ti:S lasers with fully tunable optics are now available, thus making TPE microscopy a useful tool in the biological sciences.

The main advantages of TPE microscopy are the localized excitation and accessibility to the wide range of wavelengths of most fluorophores. The limitation of two-photon excitation to the focal plane removes out-of-focus photodamage and photobleaching. This is also a method

of choice to image thick specimens due to the use of infrared light and lack of out-of-focus emission. TPE microscopy is now a standard tool for determining molecular mechanisms in basic biological research and is thus chosen for use in this study.

As a testament to the progress in the realm of microscopy, several eminent scientists have been rewarded for their impactful work. While Frits Zernike received the Nobel prize in Physics 1953 for his invention of the phase contrast microscope,[12] the 1986 prize in the same discipline was awarded to Ernst Ruska for his work in electron optics, and for designing the first electron microscope.[13] This prize was shared with Gerd Binnig and Heinrich Rohrer for designing the scanning tunneling microscope.[13] Electron microscopy provides ultra-high-resolution images of non-biological and biological specimens by using a beam of electrons as the illumination source. Due to the very short wavelength of electrons compared to photons of visible light, its resolving power is manyfold higher than the conventional microscope. The scanning tunneling microscope is capable of imaging surfaces at the atomic level. In this technique, a fine stylus is used to traverse the surface of the sample whose topography is to be studied. To avoid mechanical damage to the sample or the stylus tip, the stylus needs to be maintained at a small distance from the surface of the sample. It utilizes the principle of quantum-mechanical tunneling[14] in which an electron or other particles are able to cross an area where it cannot normally exist due to lack of high energy. Piezoelectric elements are used to control the horizontal and vertical movements of the stylus. By monitoring the current as the tip scans across the surface, information can be acquired and displayed on a monitor. Today, scanning probe microscopes are available that provide sub-nanometer optical imaging such as the atomic force microscope.

Super-resolution microscopy

More recently, the Nobel prize in Chemistry 2014 was awarded jointly to Eric Betzig, Stefan W. Hell, and William E. Moerner for the development of super-resolved fluorescence microscopy.[15] The Nobel committee noted that their ground-breaking work brought optical chemistry into the nanodimension. Stefan Hell demonstrated the method termed stimulated emission depletion (STED) microscopy while Eric Betzig and William Moerner laid the groundwork for the method, single-molecule microscopy. Hell overcame the diffraction resolution limit by using stimulated emission to inhibit the fluorescence outside the excitation regions.[16] Working separately, Moerner and Betzig used the detection of single molecules and their precise localization, and a method to precisely localize several single molecules that characterize a complex structure, respectively.[17,18] Based on the principle of single-molecule localization, photo-activated localization microscopy (PALM) and stochastic optical reconstruction microscopy (STORM) were introduced. In these techniques, photoswitchable fluorescent probes that can be turned 'on' or 'off' at will are used.[19] The sample area is imaged multiple times but each time only a few molecules are allowed to glow. The acquired images are then superimposed to yield a super-resolved image.

In 2017, the Chemistry Nobel prize was yet again awarded for work in the field of microscopy. Jacques Dubochet, Joachim Frank, and Richard Henderson were rewarded for the development of cryo-electron microscopy which enables high-resolution structure determination of biomolecules in solution.[20] Due to their discoveries, researchers can now achieve atomic resolution and routinely produce three-dimensional structures of biomolecules.

Structured illumination microscopy is a super-resolution technique based on the concept of the Moiré effect.[21] Moiré patterns are interference patterns that occur when an opaque grid pattern with transparent gaps is overlaid on another similar (but not identical) pattern. By

superimposing two patterns, one of which is the unknown sample structure and the other is a specifically structured/ patterned illumination grid, Moiré fringes are formed in the emission distribution as a result of the product of the two patterns. Since the illumination pattern is already known, the information of the fine sample structure can be recovered from the moiré. Thus, usually unresolvable high-resolution information can be obtained.

In recent times, more novel ultra-high resolution microscopy technologies have been described such as the electron-beam excitation assisted (EXA) optical microscope which combines scanning electron microscopy with its nanometric resolution and optical microscopy, thus enabling dynamic observation of living specimens.[22]

Green Fluorescent Protein

Even with the tremendous progress in the field of optical microscopy, the study of the molecular mechanisms and protein-protein interactions underlying important physiological or pathological processes wouldn't have been possible without the discovery of fluorescent proteins. The green fluorescent protein (GFP) was first isolated from the jellyfish, Aequorea Victoria in 1962.[23] The use of this protein as a labeling tool revolutionized the field of biochemistry. Researchers have since been able to visualize and study previously invisible proteins of interest. To honor their contribution to science, the Nobel prize in Chemistry 2008 was awarded to Osamu Shimomura, Martin Chalfie, and Roger Y. Tsien for the discovery and development of GFP.[24]

Green fluorescent protein is made up of 238 amino acids, has a maximal excitation wavelength with blue light at 395 nm with a minor peak at 470 nm, and emits green light with an emission maximum at 509 nm.[25] It is suitable as a fluorescent marker because of its remarkable stability and ability to form chromophores without additional cofactors. Additionally, they are non-toxic

and the function of the target protein is not affected. Over the past three decades, several lines of targeted and transgenic mice have been produced for various studies in the biological sciences. Since the turn of the century, GFP has been the marker of choice for most studies in mice since it can be visualized non-invasively and monitored in real-time in vivo or in vitro.[26] Fluorescent protein reporters thus offer advantages over enzyme-based reporters. GFP was the first example of a gene-based fluorescent protein reporter to be cloned.[27]

Since then, several mutants of the wild-type GFP gene with altered excitation and emission spectra have been described.[28] An example of such a widely used GFP variant is the enhanced GFP (EGFP), which is a red-shifted variant with a maximal excitation peak at ~490 nm. It fluoresces approximately 30-40 times brighter than the wild-type GFP when excited by blue light. Another red-shifted variant is the enhanced yellow fluorescent protein,[29] while examples of blue/ cyan emission variants are the enhanced blue fluorescent protein, and enhanced cyan fluorescent protein.[30]

In our experiments, we used commercially obtained GFP transgenic mice, generated first by Ikawa et al,[31] and bred them in-house. In these mice, GFP expression is detectable soon after birth by examining the pups under an ultraviolet lamp or fluorescent microscope. Additionally, GFP was detectable in all major organs of the body except RBC and fur. As it is seen in the lining endothelium of blood vessels, as well as platelets and WBCs, GFP mice were ideal for our experiments as we needed to make focused laser-induced injury to the endothelial lining of the blood vessels and observe thrombus formation by the adhesion and aggregation of platelets and WBCs at the injury site. GFP mice coupled with two-photon microscopy is particularly well suited for in vivo imaging experiments due to the efficient detection of fluorescent signals, better depth penetration, and minimal phototoxicity and photobleaching.[32]

Overview of hemostasis

Hemostasis is the process to prevent and stop bleeding. An ideal hemostatic response to a vessel wall injury must be quick, localized, and carefully regulated. If specific proteins of this process are absent or dysfunctional, abnormal bleeding or clotting ensues. In 1964, two proposals were independently put forward by Davie & Ratnoff,[33] and MacFarlane[34] describing a sequence of step-wise reactions involving inactive or precursor proteins circulating in the blood. This formed the basis of the intrinsic pathway of coagulation. Each of these proteins underwent minor proteolysis to become an active enzyme. Most of the steps occurred on phospholipid membrane surfaces and required calcium. Many of these proteins (clotting factors) were first identified in patients with bleeding disorders. While the intrinsic pathway was relevant to the growth and maintenance of the clotting cascade, a second pathway called the extrinsic pathway was important in the initiation of fibrin formation.[35] According to the understanding of the traditional pathways of the clotting cascade, both the extrinsic and intrinsic pathways converge on the activation of factor X (F.X) which converts prothrombin to thrombin. Thrombin then converts fibrinogen into insoluble fibrin.

However, while the classical clotting cascade has been useful in the interpretation of in vitro coagulation tests such as prothrombin time (PT) and activated partial thromboplastin time (aPTT), they raised several questions such as why factor XII deficiency did not cause bleeding, why factor XI (F.XI) deficiency caused variable symptoms and why patients with factor VIII (F.VIII) or factor IX (F.IX) deficiency had severe bleeding despite a normal extrinsic pathway.[36] To explain these aspects of hemostasis and based on knowledge generated from several years of research, scientists proposed a cell-based model of coagulation.

Cell-based model of Hemostasis

This model considers the hemostatic process to be controlled by cellular components. There are three phases of the coagulation process: initiation, amplification, and propagation.[37] The initiation happens on the surface of tissue factor (TF)-bearing cells. Depending on the procoagulant stimulus, factors Xa, IXa (a: activated), and thrombin are formed to initiate coagulation. Amplification of the process happens on the surface of platelets. As platelets adhere, aggregate, get activated, and accumulate activated cofactors on their surfaces, the procoagulant stimulus is amplified. In the final propagation phase, active proteases and their cofactors combine on the platelet surface to generate adequate amounts of thrombin.

Initiation: During hemostasis, a breach in the vessel wall enables factor VII (F.VII) in plasma to bind to cellular TF and gets rapidly activated.[38] The F.VIIa/ TF complex activates F.X and F.IX. Factor Xa can activate FV.[39] The F.Xa is rapidly inhibited by tissue factor pathway inhibitor (TFPI) or antithrombin III if it leaves the cell surface thus ensuring that the process is localized to the site of injury. However, any F.Xa remaining on the cell surface can combine with F.Va to produce small amounts of thrombin.[40]

Amplification: Injured vasculature permits platelets and plasma to come into contact with extravascular structures. These platelets get partially activated on binding with extravascular matrix proteins. The small amounts of thrombin generated in the initiation phase amplify the procoagulant signal by enhancing platelet adhesion and activation,[41] and by activation of factors V, VIII, and XI.[40] Thrombin is a potent platelet activator through the protease-activated receptors.[42] On activation, platelets release partially activated F.V from their alpha granules onto their surface.[43] This is then fully activated by thrombin or F.Xa.[39] von Willebrand factor/ FVIII complex also binds to platelets and is cleaved by thrombin to activate FVIII. Once the

activated platelets have F.Va and F.VIIIa bound on their surfaces, procoagulant complexes are manufactured and thrombin production enters the propagation phase.

Propagation: Platelets show a high binding affinity for factors IXa, Xa, and XIa.[37] In the propagation phase, the 'tenase' (F.VIIIa/ IXa) and 'prothrombinase' (F.Xa/ Va) complexes are formed on the platelet surfaces initiating large-scale thrombin production. The 'tenase' complex is formed when F.IXa reaches the platelet surface. Additionally, F.XI can bind to activated platelets and facilitate its activation by thrombin.[44] Factor XIa then provides additional F.IXa directly on the platelet surface. The 'tenase' complex activates F.X on the platelet surface and the resulting F.Xa can complex with its cofactor F.Va. This 'prothrombinase' complex now produces a significant amount of thrombin to form a fibrin clot.

Thrombosis

A clot that forms in a blood vessel is called a thrombus and the phenomenon of thrombus formation is called thrombosis. It may be considered as hemostasis occurring under the wrong circumstances. It was Rudolph Virchow[45] in 1856 who first postulated that damage to the vessel wall, alterations in blood flow, and hypercoagulability of blood are the main causes of thrombus formation. This came to be known as Virchow's triad and holds true even today. Thrombosis may occur in the arterial or venous vasculature, and the risk factors and pathophysiology differ between the two. A thrombus may occasionally dislodge from its primary site, travel through the vasculature, lodge at a distant site and occlude the vessel there. The dislodged thrombus is called an embolus and the phenomenon is known as embolism. Detailed study of the cellular and molecular mechanisms underlying thrombus formation over the past several decades has expanded on the work of Virchow.

Venous thrombosis most frequently occurs in the deep veins of the leg. Some of the risk factors for deep vein thrombosis (DVT) are immobilization, surgery, trauma, pregnancy, cancer, history of DVT, and the presence of anti-phospholipid antibodies.[46,47] Several inherited disorders with abnormalities in coagulation also render an increased risk for DVT. These include but are not limited to factor V Leiden mutation, protein C deficiency, protein S deficiency, and antithrombin deficiency.[46,47] High levels of clotting factors such as F.VIII or F.IX are also reported to be high-risk factors for venous thrombosis.[48,49] These thrombi occur in the setting of low shear stress and consist mainly of fibrin, red blood cells, and a few platelets.[46] Pulmonary embolism is a catastrophic complication of DVT in which a part or whole of the thrombus embolizes to the lung and lodges in a pulmonary artery.

Arterial thrombi are commonly formed by rupture of atherosclerotic plaques which have formed through the gradual deposition of lipid droplets and lipid-laden foamy macrophages in the arterial wall. This results in exposure to thrombogenic material such as tissue factor and the formation of a thrombus in the lumen of the blood vessel. A significantly large thrombus can occlude the artery and cause an acute coronary syndrome or a myocardial infarction.[50] When an atherosclerotic plaque ruptures, circulating platelets are recruited and form a primary hemostatic plug at the site of injury.[51] After adhesion to the injured wall with help of sub-endothelial collagen and von Willebrand factor, receptor-mediated aggregation of platelets results in the rapid growth of the thrombus, which also leads to platelet activation.[52] In both arterial and venous thrombosis, the outcome is the generation of fibrin, the main non-cellular component of the thrombus. For fibrin generation, coagulation factors in the blood interact and get activated sequentially following exposure to tissue factor.

Fibrinolysis

The process of fibrinolysis is tightly regulated by the proficient balance between activators and inhibitors of critical proteins of the hemostatic system. Plasminogen is a proenzyme with a molecular weight of 92 kDa that can be activated to initiate clot lysis.[53] Glu-plasminogen (Glu-plg), the mature isoform of plasminogen with an N-terminal glutamic acid, undergoes a conformational change from a taut structure to an activatable relaxed form through the binding of its lysine-binding site (LBS) to the carboxy-terminal lysine (CTL) residues on the surface of fibrin.[54] Tissue-type plasminogen activator (tPA) is the primary physiological activator of Glu-plg within the vasculature and is predominantly secreted from endothelial cells.[55] It activates Glu-plg to the active protease plasmin. The confluence of tPA and its substrate Glu-plg on the surface of the fibrin thrombi forms a complex that potentiates plasmin generation and facilitates fibrinolysis.[56,57] This essential step in the fibrinolytic process is kept in check by the plasma procarboxypeptidase B or procarboxypeptidase U,[58,59] also known presently as thrombin-activatable fibrinolysis inhibitor (TAFI), which is activated by thrombin-bound thrombomodulin (TM) and plasmin.[60,61] Activated TAFI (TAFIa) cleaves the CTLs from partially degraded fibrin resulting in a reduction in binding sites for the tPA-Glu-plg complex and inhibition of tPA-dependent fibrinolysis.[62]

The role of TAFI in the prolongation of clot lysis time was described in an in vitro turbidimetric assay in which a zymogen purified from plasma showed a carboxypeptidase B-like activity on activation by thrombin.[63] The thrombin-TM complex is 1250 times more capable of activating TAFI than thrombin alone.[60] As the half-life of TAFIa in plasma is ~10 minutes,[64] and there is no evidence thus far of TAFI gene-deficient mice having specific deficits of thrombosis or fibrinolysis,[65,66] the physiological relevance of the TAFI system in the regulation of fibrinolysis is not clear. Our lab, however, had previously demonstrated the influence of TM on TAFI in fibrinolysis by using an in vitro fibrin-clot model and confocal laser scanning microscopy

where supplemented soluble TM downregulated fibrinolysis by prolonging clot lysis time. That TAFI activation was responsible for this occurrence was subsequently confirmed by using TAFI-depleted plasma, a carboxypeptidase inhibitor, as well as an anti-TM neutralizing antibody, wherein soluble TM failed to prolong clot lysis time.[67] Further we had shown that endogenous TM in plasma and platelet-derived TM also activated TAFI and prevented fibrinolysis in a similar model by inhibiting Glu-plg accumulation.[68]

In the search for novel fibrinolytic agents to negate the drawbacks of current day thrombolytic drugs, inhibitors to TAFI have generated significant interest. Natural carboxypeptidase inhibitors with selective activity against TAFI but not carboxypeptidase N (a constitutively active plasma carboxypeptidase) have appealed to many investigators. Potato tuber carboxypeptidase inhibitor (PTCI) is a natural competitive inhibitor of TAFIa that binds to and penetrates the active site of the molecule, thereby blocking the substrates from accessing the active site.[69] Our lab had previously established experimental models using real-time imaging analysis[70,71] and illustrated the spatiotemporal organization of the integral elements such as platelets, Glu-plg, and fibrin within the thrombus.

AIMS & OBJECTIVES

Aim: To describe the physiological relevance of the thrombomodulin-TAFI system in the regulation of fibrinolysis using intravital imaging analysis in GFP-expressing mice.

Objectives:

1. Analyze the functional role of TAFIa and Glu-plg accumulation in vivo using labeled Glu-plg and the carboxypeptidase inhibitor PTCI.
2. Visualize and demonstrate the process of thrombolysis using rt-PA, and the effect of PTCI on rt-PA-mediated thrombolysis.

MATERIALS AND METHODS

Animals (mice)

C57BL/6-Tg (cytomegalovirus immediate early enhancer/ beta-actin promoter-enhanced green fluorescent protein) mice were purchased from SLC (Japan SLC, Inc., Shizuoka, Japan). Experiments were performed in accordance with the Japanese Law for the Humane Treatment and Management of Animals (Act No. 105; October 1973) and were approved by the Animal Experiments Committee of Hamamatsu University School of Medicine (Permit number: 2020046).

Mice were housed in a breeding room maintained between 23-26 degrees Celsius with ~50% humidity and a 12-hour light/ 12-hour dark cycle. Food and water were supplied ad libitum. Male and female mice aged between 7 and 9 weeks weighing between 15-25 grams were used for experiments.

Proteins and drugs

Glu-plasminogen was purified from fresh frozen plasma by a Lysine-Sepharose column.[72] The purified Glu-plg was labeled with Alexa Fluor 555 carboxylic acid, succinimidyl ester (Invitrogen by Thermo Fisher Scientific, Massachusetts, USA) according to the manufacturer's instructions. The labeled Glu-plg was aliquoted and stored at -80°C.

Carboxypeptidase inhibitor from potato tuber (PTCI) and epsilon aminocaproic acid (EACA) was purchased from Sigma (Saint Louis, Missouri, USA). Recombinant tissue-type Plasminogen Activator (rt-PA) was purchased from Mitsubishi Tanabe Pharma Corporation (Osaka, Japan). Doses of these agents were determined based on previous murine studies with

similar themes and were adjusted to accomplish the objectives of this study. Saline (0.9% sodium chloride solution) was used in control experiments.

Mouse preparation, laser-induced endothelial injury & thrombus generation:

Before initiating experiments, animals were anesthetized by intraperitoneal injection of a combination anesthetic agent (Medetomidine hydrochloride/ Midazolam/ Butorphanol: 0.3/ 4/ 5 mg/kg)[73] at a volume of 0.01-0.02 ml/g body weight. Four to six mice were used in each set of experiments. As the experimental procedure caused significant morbidity, the animals were euthanized (by cervical dislocation) at the conclusion of the experiments.

A 50 ul aliquot of 3 μM Glu-plg labeled with Alexa Fluor 555 (Glu-plg-AF555) was administered through retro-orbital injection of the venous sinus. The ileum was exteriorized onto a cover glass of thickness ~0.13-0.17 mm (Matsunami Glass Ind., Ltd, Japan) through a small midline vertical laparotomy incision. The mesentery of the ileum was then spread out to delineate the mesenteric blood vessels clearly and was moistened with pre-warmed saline to prevent desiccation. The prepared mouse was placed on a controllable metal heater microscope stage (ThermoPlate, Tokai Hit Co., Ltd, Japan).

In conjunction with a two-photon microscope, endothelial injury was induced by laser irradiation over a defined region of interest (ROI) measuring 19 μm^2 at the endothelial surface. The irradiation area and laser power were kept constant between experiments, and reasonably consistent thrombi were generated by altering the duration (in seconds) of the laser stimulus. Z-stack images were captured before laser stimulus and periodically after the stimulus up to a maximum of 2 hours.

Real-time imaging

All imaging experiments were performed in a dark and non-vibrating environment. The two-photon mode of a Nikon A1R MP confocal/ multiphoton microscope (Nikon Corporation, Japan) with a tunable laser (Chameleon; Coherent, Santa Clara, CA, USA) as the light source was used for intravital imaging. It was equipped with a 40X (Apochromat, Numerical Aperture 1.15) water immersion objective (Nikon Corporation, Japan) for sample visualization and laser stimulation. The mean laser power at the sample was between 60 and 80 mW, depending on the imaging depth. Image sequences were captured as 12-bit, 512 x 512-pixel images at a frame rate of 0.5 – 1 frame per second. The images were displayed in real-time on a computer monitor and saved to a hard disk. The integrated NIS-Elements software (Nikon Solutions Co., Ltd, Japan) was used to operate the microscope and process raw data. The two-photon excitation was performed at a wavelength of 1030 nm. Emitted fluorescence was split using 560-nm and 640-nm dichroic mirrors placed in series into green and red channels. They were then passed through band-pass emission filters at 525/50 nm (for GFP) and 595/50 nm (for Alexa Fluor 555) and were separately collected using GaAsP photomultiplier tubes (Hamamatsu Photonics, Shizuoka, Japan). For imaging the thrombus, up to 40 serial z-stack optical sections at 1 μm slice thickness were captured to encompass the entire thickness of the thrombus from the surface of the vessel wall to the lumen at different time points.

Investigating the Thrombomodulin-TAFI regulatory system in fibrinolysis

In these experiments, PTCI 10 mg/kg[74,75] or EACA 220 mg/kg (twice the therapeutic dose)[76] were administered through the retro-orbital route 5 mins before Glu-plg injection. After preparing the experimental set-up, 405 nm (CUBE, Coherent, CA, USA) and 561 nm (Sapphire, Coherent, CA, USA) lasers, both at 100 mW power, were used simultaneously to produce

endothelial injury and generate a thrombus. Z-stack images were captured 5 mins before and periodically after that, up to the 2-hour time point. Saline 40 µl was administered similarly in one set of experiments as a control. Fluorescence intensities were calculated and normalized to the intensity value 5 minutes before laser stimulation (pre-stimulus fluorescence intensity taken as 1).

Visualization of rt-PA-induced thrombolysis and effect of PTCI

For this group of experiments, the laser stimulus was optimized to induce endothelial injury and microthrombus formation while maintaining sensitivity to rt-PA and PTCI. A thrombus was thus generated at the endothelial surface using the 561 nm laser at 100 mW power. Thirty-five minutes later, rt-PA 3 mg/kg[71,77] was injected retro-orbitally to initiate clot lysis. A maximum of 10 minutes was taken to complete the intervention (rt-PA, PTCI injection) and resume imaging. Z-stack images were taken periodically from 5 mins before laser stimulus up to 30 mins, every 5 mins after rt-PA injection for 30 mins, and as required after that. Similar experiments were done by injecting PTCI 10 mg/kg before endothelial injury and rt-PA 30 mins after injury (pre-PTCI + rt-PA) and injecting PTCI and rt-PA together 30 mins after injury (PTCI + rt-PA). We performed control experiments by administering an equal volume of saline at the time of intervention instead of PTCI or rt-PA. Fluorescence intensities were calculated and normalized to the intensity value 5 minutes before the intervention (pre-intervention fluorescence intensity taken as 1).

Image analysis

Collated data were analyzed using the ImageJ software (National Institutes of Health and LOCI, University of Wisconsin). The information acquired over the entire depth of the thrombus was

processed using the extended depth of field plugin to generate a composite in-focus image separately for the green and red channels. A freehand ROI synchronized for all time points was charted along the border of the fluorescent areas for each of these channels (Fig. 1). The integrated density of the fluorescent area was calculated separately for each channel at the defined time points. The fluorescence intensities were normalized as described previously. Relative fluorescence intensities (RFI) were thus obtained separately for GFP and Glu-plg-AF555 at different time points. The RFIs of labeled Glu-Plg were compared between the different groups of experiments.

Fig. 1

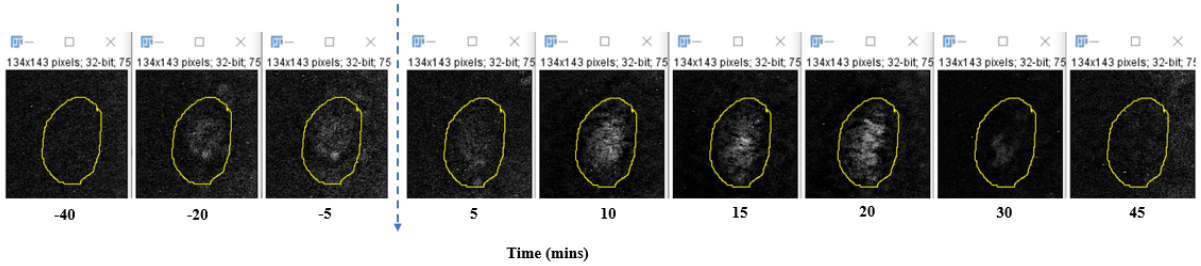

Fig. 1. Defining the region of interest (ROI) during image analysis.

Using ImageJ software, a composite in-focus grey-scale image was generated separately at each time point for both green and red channels using the Extended Depth of Field plugin and a freehand ROI synchronized to all time points was outlined followed by measurement of the fluorescence intensity.

Statistical analysis:

Descriptive statistics were presented as mean with standard deviation of Glu-plg-AF555 and GFP RFIs of the different experimental groups. Kruskal Wallis test was used to compare the difference across the groups. A post hoc pair-wise comparison was performed using the Mann Whitney U test. P-value < 0.05 was considered as statistically significant. All the analyses were carried out using R software version 4.0.4.

RESULTS

Effect of PTCI and EACA on Glu-plg accumulation

The process of microthrombi generation and progression were visualized and captured periodically for up to 120 minutes, as previously described. We observed a transient increase in the size of the thrombus in the very early phase of its formation, as evidenced by changes in GFP fluorescence intensity (Fig. 2A, B). This was in agreement with previous data from our lab in a similar experimental model.[70]

Fig. 2A

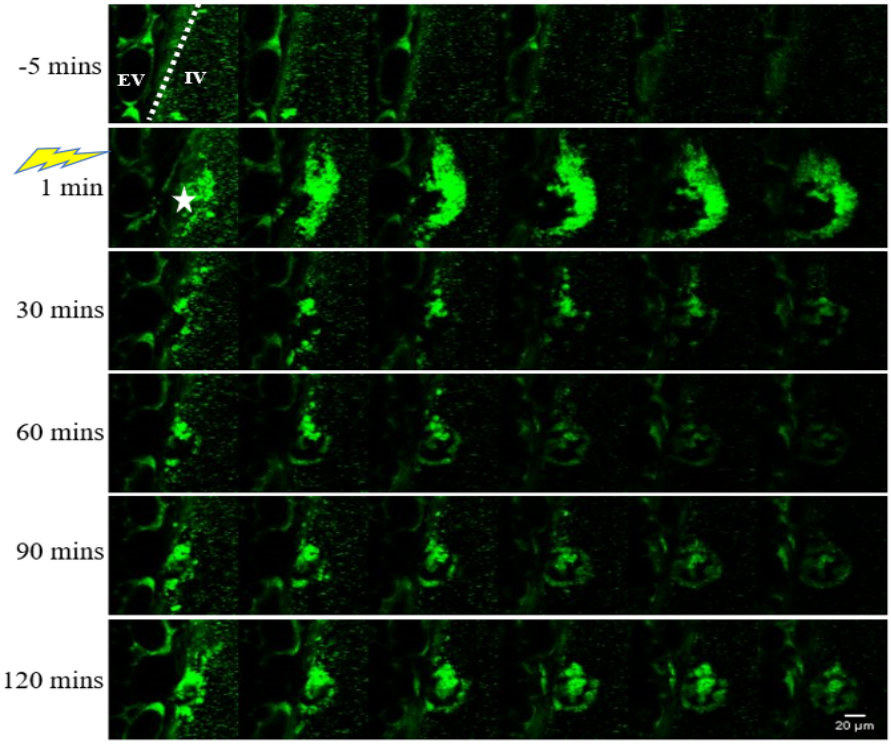

Fig. 2B

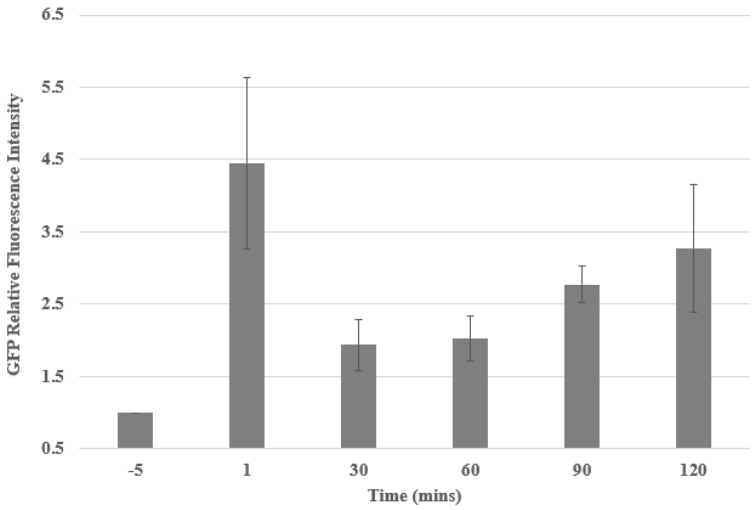

Fig. 2. Temporal changes in GFP relative fluorescence intensity (RFI) of laser-induced microthrombi.

(**A**) Representative image of microthrombus kinetics following laser injury of the vessel wall demonstrated by a montage of Z stack images. EV- extravascular, IV- intravascular, white spaced line- endothelial lining, star- site of laser injury, irregular yellow arrow- time of laser stimulus. (**B**) Temporal changes in the GFP RFI as normalized to the pre-stimulus fluorescence intensity. Mean of 3 experiments with standard deviation shown as error bars.

However, as the fluorescence of GFP could be influenced by various factors, including loss of GFP from activated platelets due to increased membrane permeability,[70] and binding and separation of WBCs and platelets to or from the thrombus, we primarily focused on the distribution and function of Glu-plg in the system over time. For this, Glu-plg-AF555 was administered to the mice to track the physiological Glu-plg in circulation. Glu-plg localized to the center of the thrombus spatiotemporally, implying that fibrinolysis is initiated at this site (Fig. 3). A peripheral shell of GFP-labeled cells comprising predominantly of platelets and few WBCs surrounded the central core of Glu-plg.

Fig. 3

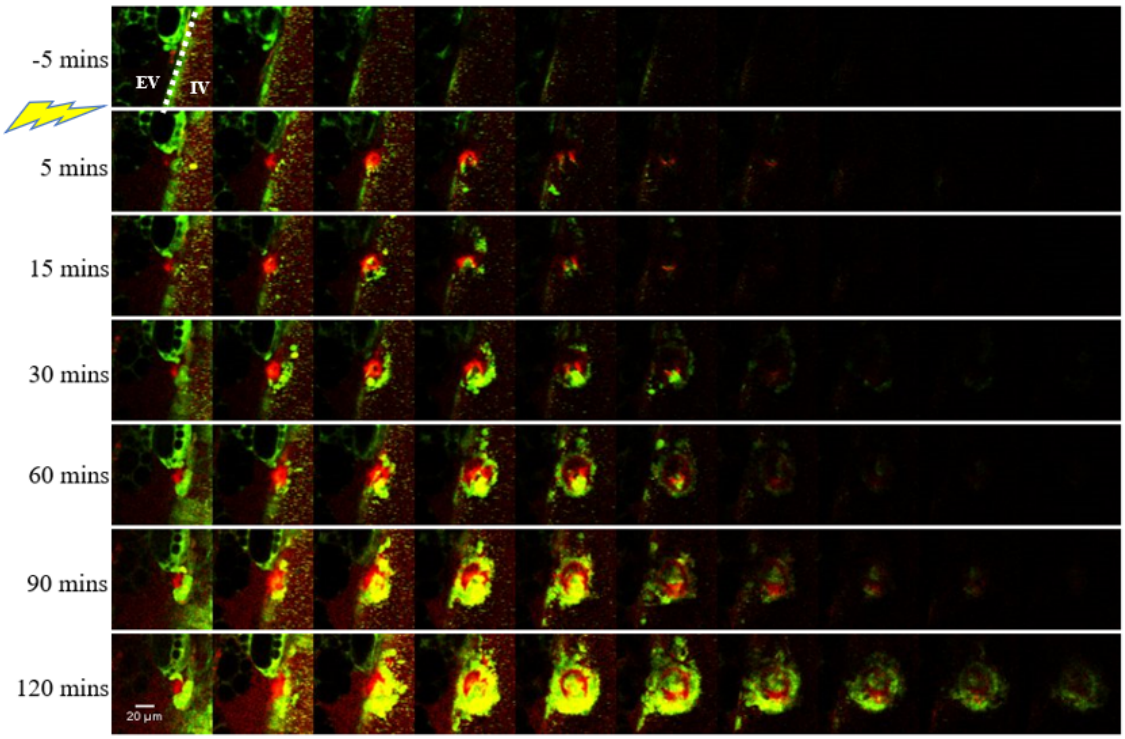

Fig. 3. Effect of PTCI on microthrombus development and Glu-plg accumulation in vivo.

Representative Z-stack images of microthrombus development over 120 minutes following laser-induced injury to the mesenteric venule endothelium of GFP mice after administration of 3 µM Glu-plg-AF555 50µl and PTCI 10mg/ kg. Glu-plg-AF555 (red) temporally accumulated at the thrombus core while GFP-expressing platelets (green) formed a covering at the periphery. EV-extravascular, IV-intravascular, white spaced line- endothelial lining, irregular yellow arrow- time of laser injury.

The extent of Glu-plg and GFP accumulation within the microthrombus differed between the control, PTCI, and EACA groups (Fig. 4A-C). The control group showed a steady increase in the RFI of Glu-plg-AF555, which was more prominent in the PTCI group but remained static in the EACA group (Fig. 4D). Analysis to compare the peak Glu-plg-AF555 RFIs between the control, PTCI, and EACA groups showed an overall statistically significant difference (P = 0.002) between the three groups. Post hoc inter-group comparison tests showed that the mean peak Glu-plg-AF555 RFIs were significantly different between each of the three groups (P = 0.008) (Fig. 4F). Together, these results show that PTCI promotes the accumulation of Glu-

plg-AF555 at the core of the thrombus by inhibiting TAFIa and primes it for lysis. EACA shows the opposite effect by blocking the binding of plasminogen to fibrin (and its subsequent conversion to plasmin).

Fig. 4

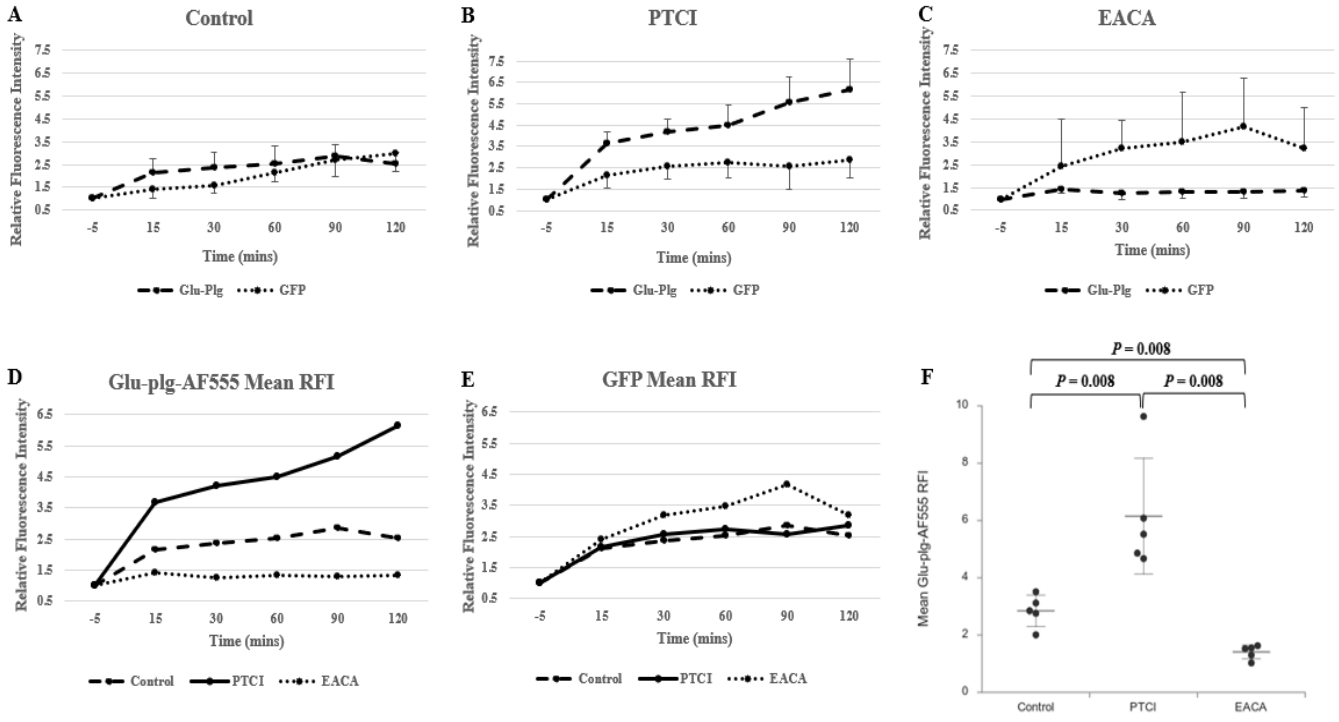

Fig. 4. Mean relative fluorescence intensity (RFI) changes of Glu-plg-AF555 and GFP over time.

The RFIs of Glu-plg-AF555 and GFP were recorded over time following laser-induced endothelial injury after administration of saline (control; **A**), PTCI (**B**), and EACA (**C**) followed by comparison between the 3 groups (**D, E).** (**F)** The peak mean Glu-plg-AF555 RFIs of the control, PTCI, and EACA groups were compared and revealed an overall statistically significant difference ($P = 0.002$). Specific inter-group differences determined by post hoc comparison analysis are shown in the figure. $P < 0.05$ taken as statistically significant. Mean ± standard deviation (error bars) of n=5 experiments each shown.

Impact of PTCI on rt-PA induced thrombolysis

The previous group of experiments demonstrated the spatiotemporal kinetics of Glu-plg-AF555 accumulation within the thrombi and the effect of PTCI and EACA on thrombus development. However, those thrombi did not lyse spontaneously over the observed period of 120 minutes. Therefore, to analyze the thrombolytic process, rt-PA 3 mg/kg was injected into the mice 35 minutes after thrombus generation. Similar experiments were done using PTCI with and without rt-PA, and control experiments using saline instead of rt-PA.

Control experiments showed no lysis up to 45 minutes after intervention (Fig. 5A). When rt-PA was given after thrombus generation (with or without PTCI), thrombolysis invariably occurred between 5-20 minutes after administering the drug (Fig. 5B). In the group where PTCI was injected before thrombus formation and rt-PA was not given (pre-PTCI only), there was no lysis till the conclusion of the experiment (Fig. 5C).

Fig. 5A

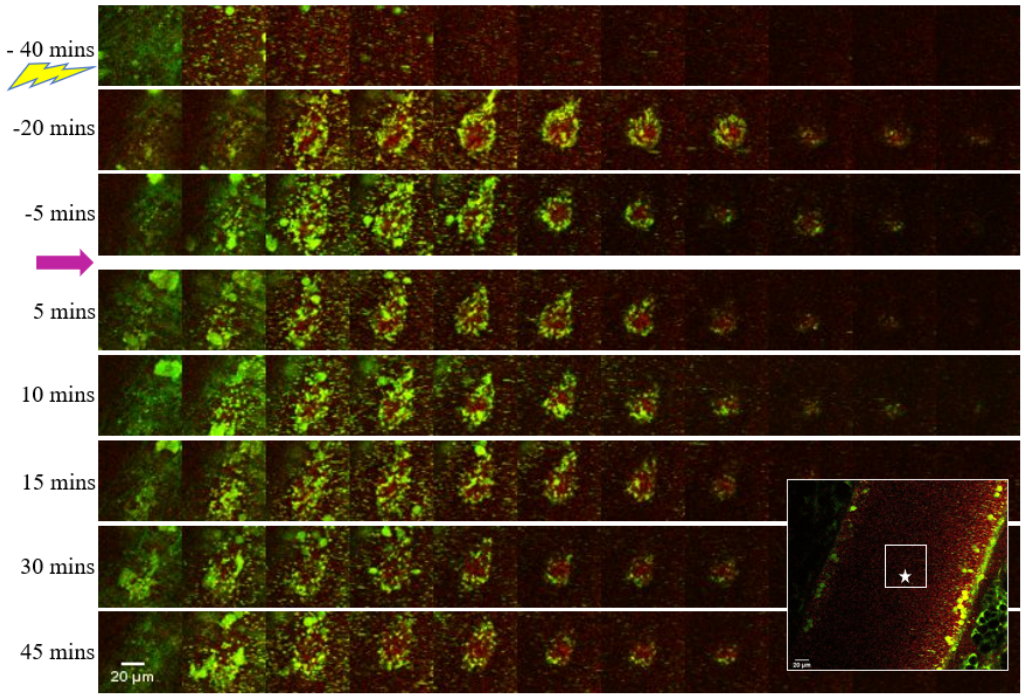

Fig. 5B

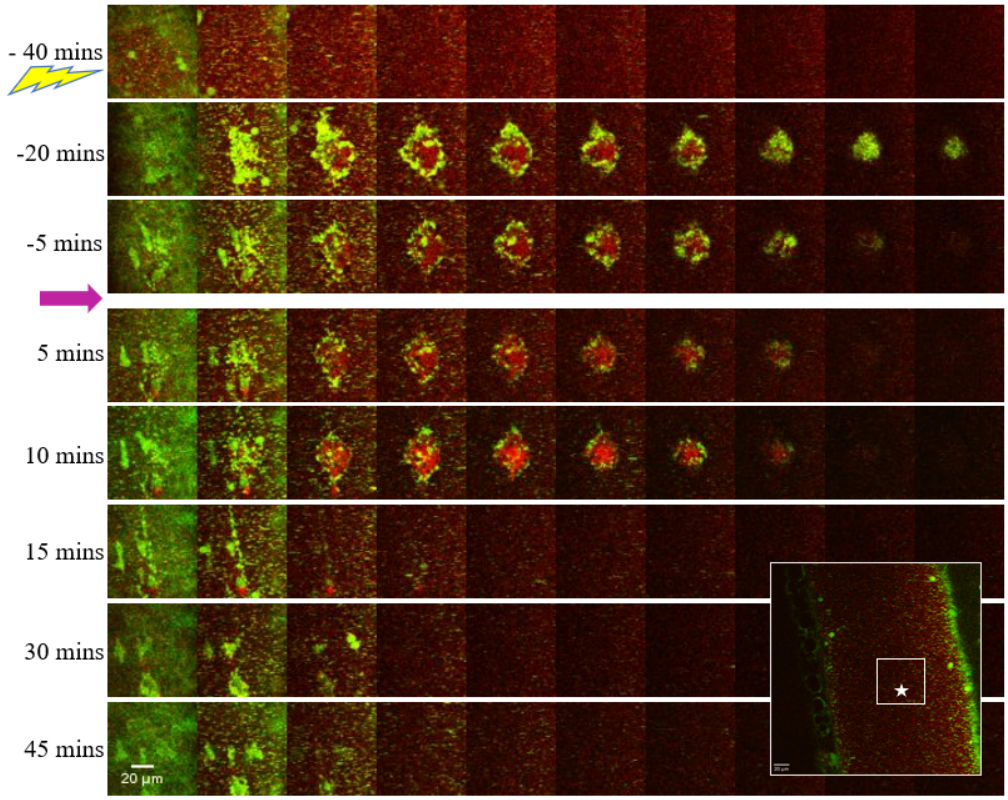
- 40 mins
-20 mins
-5 mins
5 mins
10 mins
15 mins
30 mins
45 mins
20 µm

Fig. 5C

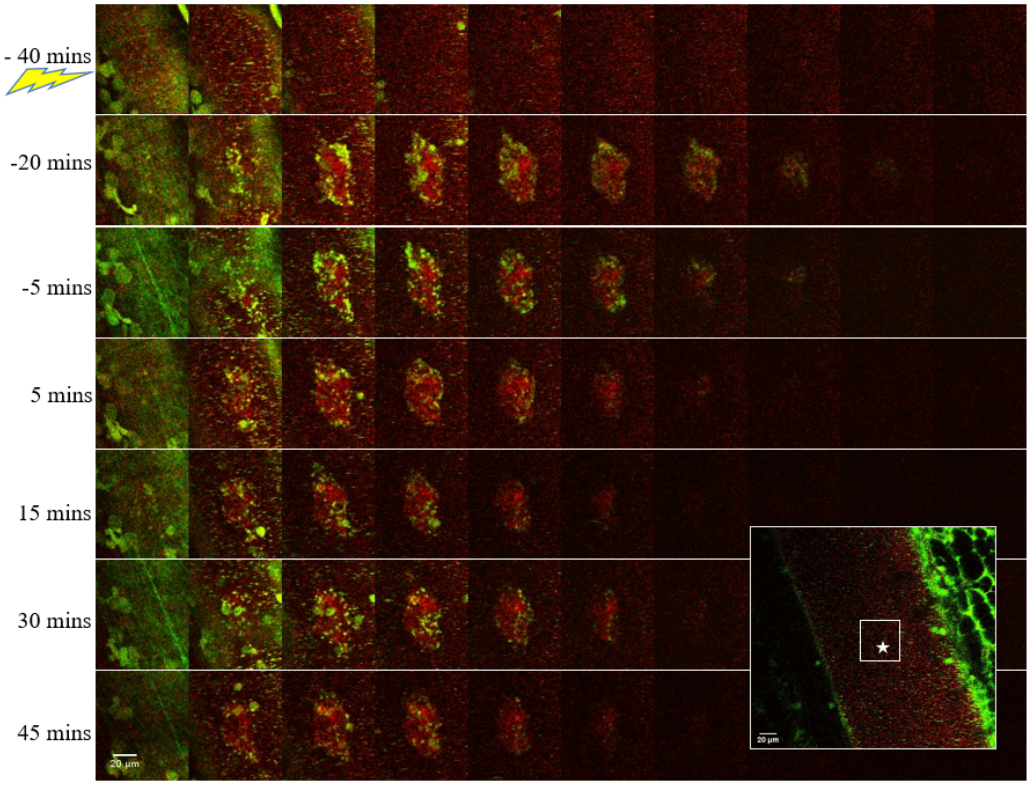
- 40 mins
-20 mins
-5 mins
5 mins
15 mins
30 mins
45 mins
20 µm

Fig. 5. Impact of PTCI and rt-PA on the fibrinolytic potential of thrombi.

Representative Z stack images of microthrombi captured from endothelial wall to luminal side before and after the injection of saline (**A**), PTCI + rt-PA (**B**), and PTCI alone (**C**). Irregular yellow arrow shows the time of laser injury, purple arrow in (A), (B) shows the intervention point. Insets- overall view of the blood vessel with the montaged region (inner square) and the point of laser stimulation at the surface of the vascular wall (star).

After administration of rt-PA, a peak increase in Glu-plg-AF555 RFIs was observed immediately before clot lysis in rt-PA only, pre-PTCI + rt-PA, and PTCI + rt-PA groups indicating impending fibrinolysis in these cases (Fig. 6A, B). In the pre-PTCI only group, the RFI increased and remained relatively stable as no clot lysis occurred. The control group showed a near baseline constant Glu-plg-AF555 RFI after saline injection (Fig. 6A, B). An early transient rise in the Glu-plg-AF555 RFI was observed immediately after laser injury in all groups due to the accelerated accumulation of Glu-plg in the developing thrombus. Similarly, a decrease in the RFIs was observed immediately following the intervention (rt-PA/ PTCI/ saline), possibly due to dilution of the protein/ dye in the system. This phenomenon is noted in the control group, whereas in the experiment groups it is offset by the effect of rt-PA/ PTCI, leading to an increase in Glu-plg RFIs until clot lysis occurs (Fig. 6B).

On comparing the time taken to achieve peak Glu-plg-AF555 RFI in these groups, a statistically significant difference was observed between the rt-PA only group, the PTCI + rt-PA group as well as the pre-PTCI + rt-PA group ($P = 0.014$). The post hoc test for multiple comparisons showed a significant difference in the time to reach peak RFI between rt-PA only and pre-PTCI + rt-PA groups ($P = 0.016$) and between the PTCI + rt-PA and pre-PTCI + rt-PA groups ($P = 0.016$). There was no statistical difference in the time to peak Glu-plg-AF555 RFI between the rt-PA only and PTCI + rt-PA groups ($P = 0.690$) (Fig. 6C). As expected, following rt-PA administration, these RFIs dropped significantly with near-complete clot lysis occurring between 15-45 minutes in all groups. Near-complete lysis time was defined as the time taken

for the Glu-plg fluorescence intensity to approximate the fluorescence intensity before the laser stimulus. A significant difference was observed in the mean time taken to achieve near-complete thrombolysis between the three groups ($P = 0.003$). Further post hoc analysis showed a significant difference between the pre-PTCI + rt-PA group compared to that of the rt-PA only and PTCI + rt-PA groups ($P = 0.008$). There was no statistically significant difference in the near-complete clot lysis times between the latter two groups ($P = 0.151$) (Fig. 6D).

Fig. 6A

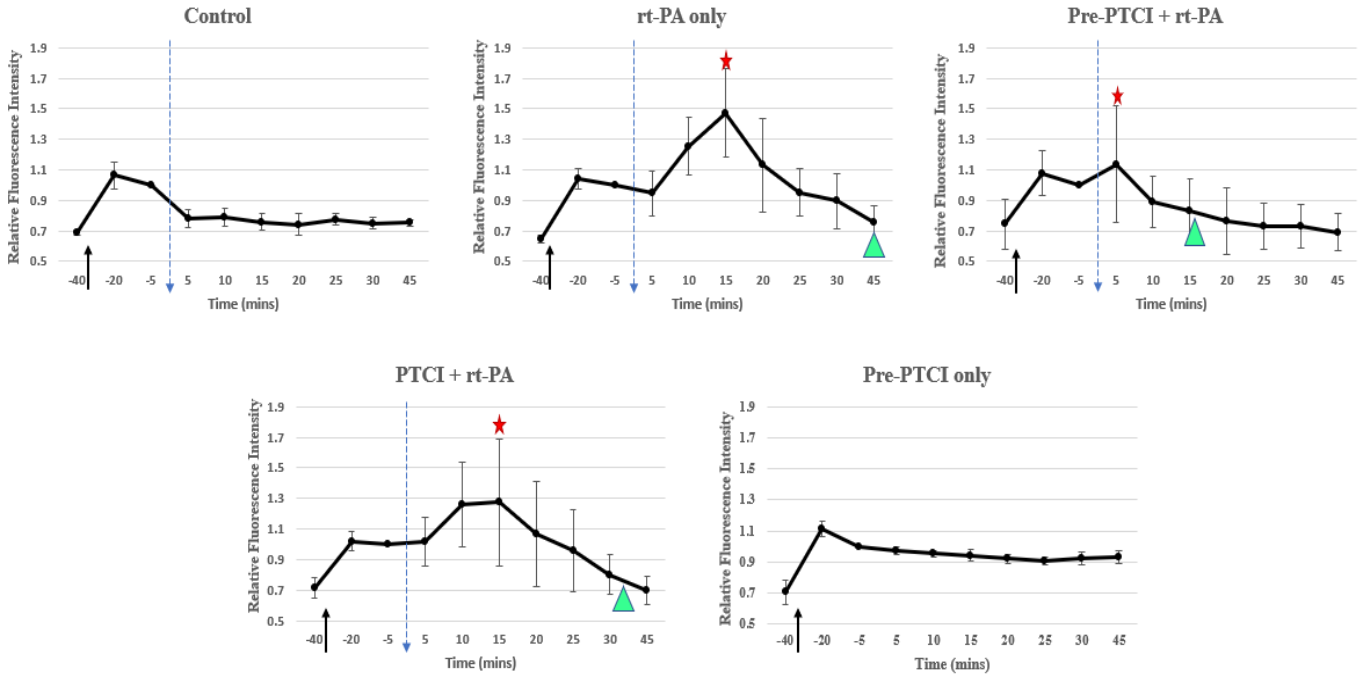

Fig. 6B

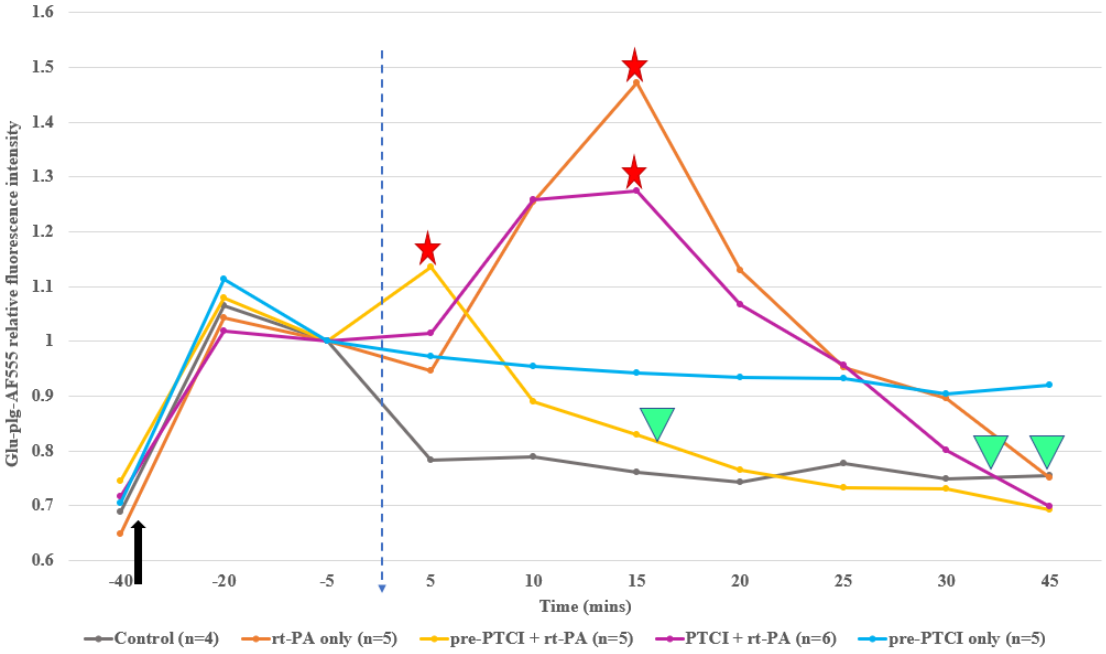

Fig. 6C

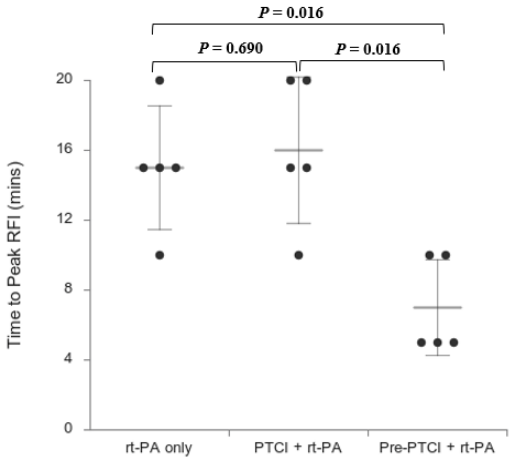

Fig. 6D

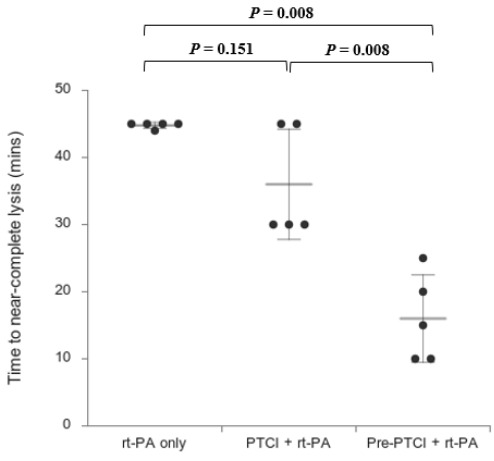

Fig. 6. Effect of rt-PA and PTCI on Glu-plg relative fluorescence intensity (RFI) changes over time.

(**A**) Mean normalized Glu-plg RFI values with standard deviation as error bars of 4-6 experiments each in all experiment groups. (**B**) Collective comparison of temporal changes in the Glu-plg-AF555 RFI between all groups. Black arrow- point of laser stimulation, blue spaced arrow- point of intervention, red stars- mean time to peak Glu-plg-AF555 RFI, green arrowheads- mean time to near-complete clot lysis. (**C-D**) The time taken to achieve peak Glu-plg-AF555 RFI (C) and near-complete clot lysis (D) were determined in experiments of rt-PA-induced fibrinolysis. Statistical analysis showed a significant difference in both parameters between the three groups displaying fibrinolysis ($P = 0.014$ and $P = 0.003$, respectively). Specific inter-group statistical differences are shown in the respective figures. $P < 0.05$ is statistically significant. Mean ± standard deviation (error bars) of n=5 experiments each.

Collectively, these results demonstrate that while spontaneous clot lysis does not occur (control experiments), exogenously administered rt-PA activates Glu-plg efficiently, leading to increased uptake within the thrombus and subsequent thrombolysis. PTCI administered in tandem with rt-PA did not expedite clot lysis compared to rt-PA administration alone, with both groups showing similar lysis patterns. However, clot lysis occurs much faster and is more efficient when the system is primed with PTCI and rt-PA is administered later (pre-PTCI + rt-PA group), as demonstrated by the faster time to reach peak Glu-plg-AF555 RFI and shorter time to attain near-complete clot lysis. Singular administration of PTCI is ineffective in thrombolysis in the absence of exogenous tPA.

DISCUSSION

In this real-time intravital imaging-based study, we used a laser-induced mouse mesenteric vein injury model to analyze the process of microthrombus formation with emphasis on Glu-plg dynamics and the effects of TAFIa on thrombolysis. We produced constant microthrombi within the mesenteric veins of GFP-expressing mice and confirmed that the TAFIa inhibitor PTCI enhanced Glu-plg accumulation at the center of the thrombi compared to saline (control) and in contrast to the antifibrinolytic agent EACA. Subsequently, we concluded that priming the mouse with PTCI augments the thrombolytic capability of rt-PA effectively compared to using rt-PA alone.

Using this model, we observed that Glu-plg is consistently concentrated at the center of the maturing thrombus. Administration of PTCI before thrombus formation led to a distinct increase in Glu-plg accumulation at the thrombus core over time, as evidenced by the rise in Glu-plg-AF555 RFI compared to control experiments. This enhanced Glu-plg binding is attributable to the removal of TAFI's inhibitory effect on fibrinolysis. Typically, LBS of Glu-plg bind to the CTLs of partially degraded fibrin in the presence of tPA, leading to its activation to plasmin. Partially degraded fibrin exposes more C-terminal basic residues due to plasmin-catalyzed cleavage, further amplifying plasmin production.[78] This endogenously generated plasmin augments Glu-plg binding in preparation for thrombolysis.[79] TAFIa down-regulates this step by cleaving the CTLs on partially degraded fibrin, effectively preventing Glu-plg binding/ activation and dampening fibrinolysis.[62] This mechanism helps stabilize immature hemostatic thrombi from premature lysis and bleeding.

EACA is a synthetic lysine analog that competitively inhibits Glu-plg accumulation in the thrombus by its affinity and blockage of LBS.[80] There was significantly less Glu-plg

accumulation when EACA was administered before laser injury compared to PTCI and control. These results show that Glu-plg accumulation in microthrombi is LBS-dependent. While EACA saturated LBS and prevented Glu-plg binding, PTCI upregulated the binding by inhibiting TAFIa and preserving the CTLs of fibrin.

GFP and platelets

Platelets form the key cellular component of microthrombi. In our experiments with GFP-expressing mice, platelets were analyzed without additional labeling by observing the changes in GFP fluorescence intensity within the thrombi over time. Compared to the control group, the EACA group showed a much higher mean GFP RFI in the first 90 minutes of observation. A decrease in platelet GFP fluorescence intensity is usually followed by phosphatidylserine exposure on the platelet surface suggesting that altered membrane permeability following platelet activation could leak GFP from the platelets.[70] Therefore, we could infer that the small thrombus size and higher RFI of GFP in the EACA group are due to decreased platelet activation. Our lab had previously shown clear colocalization of Annexin A5-labeled platelets and Glu-plg within the microthrombus, suggesting that Glu-plg accumulated at sites of platelet activation.[71] We had also demonstrated that administration of EACA showed a significant decrease in platelet binding of Glu-plg in vitro, suggesting that the surface of platelets could also be a possible source of CTLs to which binding of Glu-plg takes place.[71]

Carboxypeptidase inhibitors

There is a limited number of studies on the effects of TAFIa inhibitors to date. Although no physiological TAFI inhibitors have been described, nonspecific carboxypeptidase inhibitors such as the arginine analogs D, L-2-mercaptomethyl-3-guanidinoethylthiopropanoic acid and

guanidinoethyl-mercaptosuccinic acid have been characterized.[62,81,82] In recent years, several pharmaceutical companies have patented different low molecular weight TAFIa inhibitors, many of which have reached phases I and II of the clinical development phase.[83] However, despite early promising results, several of them were discontinued for various reasons, including but not limited to poor specificity, adverse pharmacokinetic profile, and no benefit over standard treatment.[69] To circumvent these problems, some researchers shifted their attention to developing monoclonal antibodies that target TAFI or TAFIa; however, these had issues such as poor stability, reduced binding affinity, and immunogenicity. This process was further refined by the development of bispecific antibody fragments which simultaneously target TAFI and plasminogen activator inhibitor-1, called diabodies,[84,85] and low molecular weight, low immunogenicity variable antigen-binding domains of camelid antibodies called nanobodies with excellent binding affinity, stability, and solubility.[86–88] Several of these newer inhibitors have been listed and summarized in two very insightful review articles published lately.[69,83] This line of research shows much promise in preventing and treating thrombotic diseases.

Among natural inhibitors of carboxypeptidase, only potato tuber carboxypeptidase inhibitor, tick carboxypeptidase inhibitor, and leech carboxypeptidase inhibitor have been identified as specific inhibitors of carboxypeptidase U/ TAFI.[62,89,90] PTCI is a 39 amino acid protein that competitively inhibits TAFI with an inhibitor constant (K_i) in the nanomolar range.[64] In our experiments, injection of PTCI led to prolific binding of Glu-plg at the core of the thrombus with an increase in Glu-plg-AF555 RFIs compared to control. Our lab had previously reported that phosphatidylserine exposure on the surface of platelets and fibrin formation occurs at the thrombus core.[22] Taken together, these findings emphasize the significance of this region of the thrombus and should further encourage the development of novel fibrinolytic agents targeting this site.

Laser-induced vascular injury

The availability of transgenic mice and targeted gene technology has enabled the study of the structure and function of various key molecules in several normal and pathophysiological processes. However, when studying the molecular mechanisms of hemostasis, mice models present challenges because of their small size. Vascular injury models applied in bigger animal models are many times not adaptable to the mouse. However, over the years, several murine models of vascular injury have been developed. The most common among these are mechanical injuries, electrical injuries, light-induced injuries using photoactivatable dyes, $FeCl_3$-induced injury (chemical), and laser-induced injuries.[91–93] The disadvantage of most of these methods is the involvement of surgical intervention that could artifactually activate the hemostatic system at the target site. The application of laser-induced vascular injury in conjunction with intravital imaging using two-photoexcitation microscopy circumvents this problem to some extent. The laser stimulus can be focused on a specific area of the target tissue through the microscope objective. As the energy of the laser is focused only at the focal plane of the microscope, the injury is produced only at a particular depth in the tissue. Further, the intensity of the injury can be controlled by adjusting the laser power and time of the laser stimulus.[71,93] Using this technique, injury can be consistently produced at the luminal surface of the target blood vessel and imaged in real-time.

Advantages of two-photon excitation microscopy

Two-photon excitation microscopy allows for high-resolution imaging in thick tissues such as imaging of the brain, embryos, and intra-vital imaging. The advantages of using this technology are attributed mainly to its nonlinear excitation which allows for localized excitation and a wide range of wavelengths adaptable to most fluorophores. Due to the localized excitation, there is

an increased signal-to-noise ratio. While photodamage and photobleaching outside the focal plane are significantly less, the possibility of some damage within the excitation region remains. Thus, the excitation intensity should be optimized to minimize damage to the biological system being studied. For example, the use of efficient fluorescence detectors and blanking the laser when not acquiring data could be helpful to minimize photodamage. Although the spatial resolution by TPE microscopy is very similar to confocal microscopy, the superior imaging deeper into thick samples compared to confocal microscopy is achieved mainly because of three reasons: i) there is less scattering of excitation and fluorescence emission, ii) infra-red light scatters less compared to the equivalent visible or blue-green light, and iii) since two-photon excitation is limited to the focal plane, no excitation light will be absorbed and more light reaches the focus.[94]

Effect of TAFI and PTCI on rt-PA-induced fibrinolysis

When we investigated the effects of TAFIa on thrombolysis using TPE microscopy, the results varied depending on the time of administration of PTCI and the presence or absence of exogenous rt-PA. As these were short-duration experiments, we injected rt-PA as a single bolus dose 35 minutes after thrombus formation. Glu-plg-AF555 was administered to evaluate how exogenous rt-PA influenced Glu-plg accumulation and fibrinolysis in vivo. As expected, solitary administration of rt-PA after thrombus formation caused thrombolysis, while control experiments showed no lysis for the entire experiment duration. Sole administration of PTCI did not cause lysis. While we predicted accelerated clot lysis on co-administration of PTCI with rt-PA, the thrombolysis patterns between rt-PA administration alone and co-administration of PTCI with rt-PA were more or less similar, with both groups reaching a peak Glu-plg-AF555 RFI intensity between 10-15 minutes after the drug/ protein injection, followed

by lysis. However, when PTCI was administered before laser endothelial injury and rt-PA was administered 35 minutes after thrombus formation, there was a brisk increase in Glu-plg-AF555 intensity within 5 minutes of rt-PA administration followed by lysis. In this instance, near-complete thrombolysis also occurred significantly faster than rt-PA administration alone and co-administration of PTCI with rt-PA. Notably, PTCI by itself could also cause a similar increase in Glu-plg fluorescence intensity attributable to TAFI inhibition and ensuing Glu-plg accumulation, albeit with no subsequent decrease in fluorescence as lysis does not occur. Satisfactory systemic inhibition of TAFIa at an earlier phase before thrombolytic therapy by tPA seems relevant to obtain effective enhancement of thrombolysis.

Few studies have previously explicitly investigated the effect of PTCI on clot lysis in vitro or in vivo. In a rabbit arterial thrombolysis model, Klement et al. showed that injection of PTCI alone did not induce clot lysis in the absence of exogenous tPA. In contrast, PTCI enhanced tPA-induced clot lysis in vivo and ex vivo.[95] In a rabbit jugular vein thrombolysis model, Minnema et al. gave evidence of increased clot lysis using PTCI in the absence of tPA.[96] However, using the same model, Nagashima et al. demonstrated increased thrombolytic potency of tPA by systemic co-administration of PTCI. At the same time, there was no endogenous fibrinolysis by administration of PTCI alone in the absence of tPA.[97] This discrepancy was attributed to the difference in the concentration and time of administration of PTCI between the two studies. Muto et al. concluded that PTCI did not affect clot formation and dose-dependently enhanced tPA-induced clot lysis both in vitro and ex vivo using rat plasma in addition to showing strong antithrombotic effects in a tissue factor-induced renal microthrombosis model in vivo.[98] In a murine ferric chloride-induced vena cava thrombosis model, Wang et al. demonstrated a maximum decrease in thrombus size up to 45% using PTCI alone without exogenous tPA administration.[75] Finally, Bird et al. used three different models of thrombosis in rats and showed that PTCI was ineffective in thrombolysis without tPA.[74]

Despite using different experimental models, most of these studies endorse the fact that PTCI enhances the thrombolytic potential of tPA, which agrees with our findings. Whether PTCI can induce clot lysis in the absence of exogenous tPA is, however, not yet clear as the data on this front is conflicting.

Conclusions:

We used a multiphoton microscope-based murine in vivo microthrombus imaging model to visualize and establish in real-time the physiological relevance of TAFI in the regulation of fibrinolysis. The TAFIa inhibitor PTCI appeared to enhance Glu-plg accumulation at the center of the thrombi. Further, pre-administration rather than co-administration of PTCI with rt-PA showed a distinct benefit, with faster lysis time and earlier near-complete thrombolysis. Based on our findings and understanding of the spatiotemporal regulatory mechanism of thrombolysis, we reiterate that PTCI, and TAFI inhibitors in general, show great promise in the management of thrombotic diseases. More studies are needed to assess the pharmacokinetic and pharmacodynamic profile of this group of drugs for potential use in thrombolysis or thromboprophylaxis.

Limitations:

As we used only a single constant dose of all drugs and proteins in this study, it is limited by the absence of data on dose-dependent variations, particularly on the effects of PTCI and rt-PA on thrombus formation and lysis. Additionally, testing more time points of PTCI administration could have further substantiated the findings of this study.

Acknowledgments:

The fluorescence imaging experiments were performed at the Advanced Research Facilities & Services, Hamamatsu University School of Medicine.

Sources of funding:

This work was supported by AMED under Grant Number JP21ek0210154 to Dr. Tetsumei Urano and Dr. Yuko Suzuki (Professors, Department of Medical Physiology, Hamamatsu University School of Medicine), JSPS KAKENHI Grant Number JP19K08577 to Dr. Yuko Suzuki, a grant from the Smoking Research Foundation to Dr. Tetsumei Urano and Dr. Yuko Suzuki, and Grants-in-Aid from Hamamatsu University School of Medicine to Dr. Nitty Skariah Mathews.

Disclosures: None

References:

1. Global Health Estimates: Life expectancy and leading causes of death and disability. Accessed September 10, 2021. https://www.who.int/data/gho/data/themes/mortality-and-global-health-estimates

2. Berkowitz SD, Granger CB, Pieper KS, et al. Incidence and predictors of bleeding after contemporary thrombolytic therapy for myocardial infarction. The Global Utilization of Streptokinase and Tissue Plasminogen activator for Occluded coronary arteries (GUSTO) I Investigators. *Circulation*. 1997;95(11):2508-2516. doi:10.1161/01.cir.95.11.2508

3. Emberson J, Lees KR, Lyden P, et al. Effect of treatment delay, age, and stroke severity on the effects of intravenous thrombolysis with alteplase for acute ischaemic stroke: a meta-analysis of individual patient data from randomised trials. *Lancet Lond Engl*. 2014;384(9958):1929-1935. doi:10.1016/S0140-6736(14)60584-5

4. Abbe E. Beiträge zur Theorie des Mikroskops und der mikroskopischen Wahrnehmung. *Arch Für Mikrosk Anat*. 1873;9(1):413-468.

5. Garini Y, Vermolen BJ, Young IT. From micro to nano: recent advances in high-resolution microscopy. *Curr Opin Biotechnol*. 2005;16(1):3-12. doi:10.1016/j.copbio.2005.01.003

6. Meilan PF, Garavaglia M. Rayleigh criterion of resolution and light sources of different spectral composition. In: *Fifth International Topical Meeting on Education and Training in Optics*. Vol 3190. SPIE; 1997:296-303. doi:10.1117/12.294397

7. Mansuripur M. Distribution of light at and near the focus of high-numerical-aperture objectives. *JOSA A*. 1986;3(12):2086-2093. doi:10.1364/JOSAA.3.002086

8. Marvin Minsky,. Accessed January 17, 2022. https://web.media.mit.edu/~minsky/papers/ConfocalMemoir.html

9. Nwaneshiudu A, Kuschal C, Sakamoto FH, Rox Anderson R, Schwarzenberger K, Young RC. Introduction to confocal microscopy. *J Invest Dermatol*. 2012;132(12):1-5. doi:10.1038/jid.2012.429

10. Göppert-Mayer M. Über Elementarakte mit zwei Quantensprüngen. *Ann Phys*. 1931;401(3):273-294. doi:10.1002/andp.19314010303

11. Denk W, Strickler JH, Webb WW. Two-Photon Laser Scanning Fluorescence Microscopy. *Science*. Published online April 6, 1990. doi:10.1126/science.2321027

12. The Nobel Prize in Physics 1953. NobelPrize.org. Accessed January 14, 2022. https://www.nobelprize.org/prizes/physics/1953/summary/

13. The Nobel Prize in Physics 1986. NobelPrize.org. Accessed January 14, 2022. https://www.nobelprize.org/prizes/physics/1986/summary/

14. scanning tunneling microscope | instrument | Britannica. Accessed January 18, 2022. https://www.britannica.com/technology/scanning-tunneling-microscope

15. The Nobel Prize in Chemistry 2014. NobelPrize.org. Accessed January 14, 2022. https://www.nobelprize.org/prizes/chemistry/2014/summary/

16. Hell SW, Wichmann J. Breaking the diffraction resolution limit by stimulated emission: stimulated-emission-depletion fluorescence microscopy. *Opt Lett*. 1994;19(11):780-782. doi:10.1364/OL.19.000780

17. Moerner WE. Examining Nanoenvironments in Solids on the Scale of a Single, Isolated Impurity Molecule. *Science*. Published online July 1, 1994. doi:10.1126/science.265.5168.46

18. Betzig E, Patterson GH, Sougrat R, et al. Imaging Intracellular Fluorescent Proteins at Nanometer Resolution. *Science*. Published online September 15, 2006. doi:10.1126/science.1127344

19. Yamanaka M, Smith NI, Fujita K. Introduction to super-resolution microscopy. *Microscopy*. 2014;63(3):177-192. doi:10.1093/jmicro/dfu007

20. The Nobel Prize in Chemistry 2017. NobelPrize.org. Accessed January 14, 2022. https://www.nobelprize.org/prizes/chemistry/2017/press-release/

21. Surpassing the lateral resolution limit by a factor of two using structured illumination microscopy - Gustafsson - 2000 - Journal of Microscopy - Wiley Online Library.

Accessed January 14, 2022. https://onlinelibrary.wiley.com/doi/full/10.1046/j.1365-2818.2000.00710.x

22. Inami W, Nakajima K, Miyakawa A, Kawata Y. Electron beam excitation assisted optical microscope with ultra-high resolution. *Opt Express*. 2010;18(12):12897-12902. doi:10.1364/OE.18.012897

23. Shimomura O, Johnson FH, Saiga Y. Extraction, Purification and Properties of Aequorin, a Bioluminescent Protein from the Luminous Hydromedusan, Aequorea. *J Cell Comp Physiol*. 1962;59(3):223-239. doi:10.1002/jcp.1030590302

24. The Nobel Prize in Chemistry 2008. NobelPrize.org. Accessed January 16, 2022. https://www.nobelprize.org/prizes/chemistry/2008/press-release/

25. Chalfie M, Tu Y, Euskirchen G, Ward WW, Prasher DC. Green Fluorescent Protein as a Marker for Gene Expression. *Science*. Published online February 11, 1994. doi:10.1126/science.8303295

26. Hadjantonakis AK, Nagy A. The color of mice: in the light of GFP-variant reporters. *Histochem Cell Biol*. 2001;115(1):49-58. doi:10.1007/s004180000233

27. Prasher DC, Eckenrode VK, Ward WW, Prendergast FG, Cormier MJ. Primary structure of the Aequorea victoria green-fluorescent protein. *Gene*. 1992;111(2):229-233. doi:10.1016/0378-1119(92)90691-H

28. Cormack BP, Valdivia RH, Falkow S. FACS-optimized mutants of the green fluorescent protein (GFP). *Gene*. 1996;173(1):33-38. doi:10.1016/0378-1119(95)00685-0

29. Ormö M, Cubitt AB, Kallio K, Gross LA, Tsien RY, Remington SJ. Crystal Structure of the Aequorea victoria Green Fluorescent Protein. *Science*. Published online September 6, 1996. doi:10.1126/science.273.5280.1392

30. Heim R, Tsien RY. Engineering green fluorescent protein for improved brightness, longer wavelengths and fluorescence resonance energy transfer. *Curr Biol*. 1996;6(2):178-182. doi:10.1016/S0960-9822(02)00450-5

31. Ikawa M, Kominami K, Yoshimura Y, Tanaka K, Nishimune Y, Okabe M. Green fluorescent protein as a marker in transgenic mice. *Dev Growth Differ*. 1995;37(4):455-459. doi:10.1046/j.1440-169X.1995.t01-2-00012.x

32. Mainen ZF, Maletic-Savatic M, Shi SH, Hayashi Y, Malinow R, Svoboda K. Two-Photon Imaging in Living Brain Slices. *Methods*. 1999;18(2):231-239. doi:10.1006/meth.1999.0776

33. Davie EW, Ratnoff OD. Waterfall Sequence for Intrinsic Blood Clotting. *Science*. Published online September 18, 1964. doi:10.1126/science.145.3638.1310

34. Macfarlane RG. An Enzyme Cascade in the Blood Clotting Mechanism, and its Function as a Biochemical Amplifier. *Nature*. 1964;202(4931):498-499. doi:10.1038/202498a0

35. Davie EW, Fujikawa K, Kisiel W. The coagulation cascade: initiation, maintenance, and regulation. ACS Publications. doi:10.1021/bi00107a001

36. Gailani D, Renné T. The intrinsic pathway of coagulation: a target for treating thromboembolic disease? *J Thromb Haemost*. 2007;5(6):1106-1112. doi:10.1111/j.1538-7836.2007.02446.x

37. Hoffman M, Iii DMM. A Cell-based Model of Hemostasis. *Thromb Haemost*. 2001;85(6):958-965. doi:10.1055/s-0037-1615947

38. Wildgoose P, Kisiel W. Activation of human factor VII by factors IXa and Xa on human bladder carcinoma cells. *Blood*. 1989;73(7):1888-1895. doi:10.1182/blood.V73.7.1888.1888

39. Monkovic DD, Tracy PB. Activation of human factor V by factor Xa and thrombin. ACS Publications. doi:10.1021/bi00457a004

40. Monroe D, Hoffman M, Roberts H. Transmission of a procoagulant signal from tissue factor-bearing cell to platelets. *Blood Coagul Fibrinolysis Int J Haemost Thromb*. 1996;7:459-464.

41. Diaz-Ricart M, Estebanell E, Lozano M, et al. Thrombin facilitates primary platelet adhesion onto vascular surfaces in the absence of plasma adhesive proteins: studies under flow conditions. *Haematologica*. 2000;85(3):280-288. doi:10.3324/%x

42. Hung DT, Vu TK, Wheaton VI, Ishii K, Coughlin SR. Cloned platelet thrombin receptor is necessary for thrombin-induced platelet activation. *J Clin Invest*. 1992;89(4):1350-1353. doi:10.1172/JCI115721

43. Monković DD, Tracy PB. Functional characterization of human platelet-released factor V and its activation by factor Xa and thrombin. *J Biol Chem*. 1990;265(28):17132-17140. doi:10.1016/S0021-9258(17)44879-4

44. Oliver JA, Monroe DM, Roberts HR, Hoffman M. Thrombin Activates Factor XI on Activated Platelets in the Absence of Factor XII. *Arterioscler Thromb Vasc Biol*. 1999;19(1):170-177. doi:10.1161/01.ATV.19.1.170

45. VIRCHOW R. Phlogose und thrombose in gefassystem. *Gesammelte Abh Zur Wiss Med*. Published online 1856:458-463.

46. Kyrle PA, Eichinger S. Deep vein thrombosis. *The Lancet*. 2005;365(9465):1163-1174. doi:10.1016/S0140-6736(05)71880-8

47. Rosendaal F. Venous thrombosis: a multicausal disease. *The Lancet*. 1999;353(9159):1167-1173. doi:10.1016/S0140-6736(98)10266-0

48. Koster T, Vandenbroucke JP, Rosendaal FR, Briët E, Rosendaal FR, Blann AD. Role of clotting factor VIII in effect of von Willebrand factor on occurrence of deep-vein thrombosis. *The Lancet*. 1995;345(8943):152-155. doi:10.1016/S0140-6736(95)90166-3

49. Vlieg A van H, van der Linden IK, Bertina RM, Rosendaal FR. High levels of factor IX increase the risk of venous thrombosis. *Blood*. 2000;95(12):3678-3682. doi:10.1182/blood.V95.12.3678

50. Rader DJ, Daugherty A. Translating molecular discoveries into new therapies for atherosclerosis. *Nature*. 2008;451(7181):904-913. doi:10.1038/nature06796

51. Ruggeri ZM, Mendolicchio GL. Adhesion Mechanisms in Platelet Function. *Circ Res*. 2007;100(12):1673-1685. doi:10.1161/01.RES.0000267878.97021.ab

52. Mackman N. Triggers, targets and treatments for thrombosis. *Nature*. 2008;451(7181):914-918. doi:10.1038/nature06797

53. Lijnen HR, Collen D. 1 Mechanisms of physiological fibrinolysis. *Baillières Clin Haematol*. 1995;8(2):277-290. doi:10.1016/S0950-3536(05)80268-9

54. Rijken DC, Lijnen HR. New insights into the molecular mechanisms of the fibrinolytic system. *J Thromb Haemost*. 2009;7(1):4-13. doi:10.1111/j.1538-7836.2008.03220.x

55. Urano T, Suzuki Y, Iwaki T, Sano H, Honkura N, Castellino FJ. Recognition of Plasminogen Activator Inhibitor Type 1 as the Primary Regulator of Fibrinolysis. *Curr Drug Targets*. 2019;20(16):1695-1701. doi:10.2174/1389450120666190715102510

56. Gebbink MFBG. Tissue-type plasminogen activator-mediated plasminogen activation and contact activation, implications in and beyond haemostasis. *J Thromb Haemost*. 2011;9(s1):174-181. doi:10.1111/j.1538-7836.2011.04278.x

57. Urano T, Castellino FJ, Suzuki Y. Regulation of plasminogen activation on cell surfaces and fibrin. *J Thromb Haemost*. 2018;16(8):1487-1497. doi:10.1111/jth.14157

58. Eaton DL, Malloy BE, Tsai SP, Henzel W, Drayna D. Isolation, molecular cloning, and partial characterization of a novel carboxypeptidase B from human plasma. *J Biol Chem*. 1991;266(32):21833-21838.

59. Hendriks D, Scharpé S, van Sande M, Lommaert MP. Characterisation of a carboxypeptidase in human serum distinct from carboxypeptidase N. *J Clin Chem Clin Biochem Z Klin Chem Klin Biochem*. 1989;27(5):277-285. doi:10.1515/cclm.1989.27.5.277

60. Bajzar L, Morser J, Nesheim M. TAFI, or Plasma Procarboxypeptidase B, Couples the Coagulation and Fibrinolytic Cascades through the Thrombin-Thrombomodulin Complex. *J Biol Chem*. 1996;271(28):16603-16608. doi:10.1074/jbc.271.28.16603

61. Mao SS, Cooper CM, Wood T, Shafer JA, Gardell SJ. Characterization of plasmin-mediated activation of plasma procarboxypeptidase B. Modulation by glycosaminoglycans. *J Biol Chem*. 1999;274(49):35046-35052. doi:10.1074/jbc.274.49.35046

62. Redlitz A, Tan AK, Eaton DL, Plow EF. Plasma carboxypeptidases as regulators of the plasminogen system. *J Clin Invest*. 1995;96(5):2534-2538.

63. Bajzar L, Manuel R, Nesheim ME. Purification and Characterization of TAFI, a Thrombin-activable Fibrinolysis Inhibitor ∗. *J Biol Chem*. 1995;270(24):14477-14484. doi:10.1074/jbc.270.24.14477

64. Boffa MB, Wang W, Bajzar L, Nesheim ME. Plasma and Recombinant Thrombin-activable Fibrinolysis Inhibitor (TAFI) and Activated TAFI Compared with Respect to Glycosylation, Thrombin/Thrombomodulin-dependent Activation, Thermal Stability, and Enzymatic Properties *. *J Biol Chem*. 1998;273(4):2127-2135. doi:10.1074/jbc.273.4.2127

65. Morser J, Gabazza EC, Myles T, Leung LLK. What has been learnt from the thrombin-activatable fibrinolysis inhibitor-deficient mouse? *J Thromb Haemost*. 2010;8(5):868-876. doi:10.1111/j.1538-7836.2010.03787.x

66. Leung LLK, Morser J. Carboxypeptidase B2 and carboxypeptidase N in the crosstalk between coagulation, thrombosis, inflammation, and innate immunity. *J Thromb Haemost*. 2018;16(8):1474-1486. doi:10.1111/jth.14199

67. Brzoska T, Suzuki Y, Sano H, et al. Imaging analyses of coagulation-dependent initiation of fibrinolysis on activated platelets and its modification by thrombin-activatable fibrinolysis inhibitor. *Thromb Haemost*. 2017;117(4):682-690. doi:10.1160/TH16-09-0722

68. Suzuki Y, Sano H, Mochizuki L, Honkura N, Urano T. Activated platelet-based inhibition of fibrinolysis via thrombin-activatable fibrinolysis inhibitor activation system. *Blood Adv*. 2020;4(21):5501-5511. doi:10.1182/bloodadvances.2020002923

69. Sillen M, Declerck PJ. Thrombin Activatable Fibrinolysis Inhibitor (TAFI): An Updated Narrative Review. *Int J Mol Sci*. 2021;22(7):3670. doi:10.3390/ijms22073670

70. Hayashi T, Mogami H, Murakami Y, et al. Real-time analysis of platelet aggregation and procoagulant activity during thrombus formation in vivo. *Pflüg Arch - Eur J Physiol*. 2008;456(6):1239-1251. doi:10.1007/s00424-008-0466-9

71. Brzoska T, Tanaka-Murakami A, Suzuki Y, Sano H, Kanayama N, Urano T. Endogenously generated plasmin at the vascular wall injury site amplifies lysine binding site-dependent plasminogen accumulation in microthrombi. *PloS One*. 2015;10(3):e0122196. doi:10.1371/journal.pone.0122196

72. Deutsch DG, Mertz ET. Plasminogen: Purification from Human Plasma by Affinity Chromatography. *Science*. 1970;170(3962):1095-1096. doi:10.1126/science.170.3962.1095

73. Kawai S, Takagi Y, Kaneko S, Kurosawa T. Effect of Three Types of Mixed Anesthetic Agents Alternate to Ketamine in Mice. *Exp Anim*. 2011;60(5):481-487. doi:10.1538/expanim.60.481

74. Bird E, Tamura J, Bostwick JS, et al. Is exogenous tissue plasminogen activator necessary for antithrombotic efficacy of an inhibitor of thrombin activatable fibrinolysis inhibitor (TAFI) in rats? *Thromb Res*. 2007;120(4):549-558. doi:10.1016/j.thromres.2006.11.010

75. Wang X, Smith PL, Hsu MY, Ogletree ML, Schumacher WA. Murine model of ferric chloride-induced vena cava thrombosis: evidence for effect of potato carboxypeptidase inhibitor. *J Thromb Haemost JTH*. 2006;4(2):403-410. doi:10.1111/j.1538-7836.2006.01703.x

76. Singh S, Houng AK, Reed GL. Venous stasis-induced fibrinolysis prevents thrombosis in mice: role of α2-antiplasmin. *Blood*. 2019;134(12):970-978. doi:10.1182/blood.2019000049

77. Singh S, Houng A, Reed GL. Releasing the Brakes on the Fibrinolytic System in Pulmonary Emboli. *Circulation*. 2017;135(11):1011-1020. doi:10.1161/CIRCULATIONAHA.116.024421

78. Suenson E, Lützen O, Thorsen S. Initial plasmin-degradation of fibrin as the basis of a positive feed-back mechanism in fibrinolysis. *Eur J Biochem*. 1984;140(3):513-522. doi:10.1111/j.1432-1033.1984.tb08132.x

79. Suzuki Y, Yasui H, Brzoska T, Mogami H, Urano T. Surface-retained tPA is essential for effective fibrinolysis on vascular endothelial cells. *Blood*. 2011;118(11):3182-3185. doi:10.1182/blood-2011-05-353912

80. Markus G, DePasquale JL, Wissler FC. Quantitative determination of the binding of epsilon-aminocaproic acid to native plasminogen. *J Biol Chem*. 1978;253(3):727-732. doi:10.1016/S0021-9258(17)38163-2

81. Wang W, Hendriks DF, Scharpé SS. Carboxypeptidase U, a plasma carboxypeptidase with high affinity for plasminogen. *J Biol Chem*. 1994;269(22):15937-15944. doi:10.1016/S0021-9258(17)40771-X

82. Mao SS, Colussi D, Bailey CM, et al. Electrochemiluminescence assay for basic carboxypeptidases: inhibition of basic carboxypeptidases and activation of thrombin-activatable fibrinolysis inhibitor. *Anal Biochem*. 2003;319(1):159-170. doi:10.1016/S0003-2697(03)00252-5

83. Claesen K, Mertens JC, Leenaerts D, Hendriks D. Carboxypeptidase U (CPU, TAFIa, CPB2) in Thromboembolic Disease: What Do We Know Three Decades after Its Discovery? *Int J Mol Sci*. 2021;22(2):883. doi:10.3390/ijms22020883

84. Develter J, Booth NA, Declerck PJ, Gils A. Bispecific targeting of thrombin activatable fibrinolysis inhibitor and plasminogen activator inhibitor-1 by a heterodimer diabody. *J Thromb Haemost JTH*. 2008;6(11):1884-1891. doi:10.1111/j.1538-7836.2008.03137.x

85. Wyseure T, Gils A, Declerck PJ. Evaluation of the profibrinolytic properties of a bispecific antibody-based inhibitor against human and mouse thrombin-activatable fibrinolysis inhibitor and plasminogen activator inhibitor-1. *J Thromb Haemost*. 2013;11(11):2069-2071. doi:10.1111/jth.12399

86. Hamers-Casterman C, Atarhouch T, Muyldermans S, et al. Naturally occurring antibodies devoid of light chains. *Nature*. 1993;363(6428):446-448. doi:10.1038/363446a0

87. Muyldermans S. Single domain camel antibodies: current status. *Rev Mol Biotechnol*. 2001;74(4):277-302. doi:10.1016/S1389-0352(01)00021-6

88. Buelens K, Hassanzadeh-Ghassabeh G, Muyldermans S, Gils A, Declerck PJ. Generation and characterization of inhibitory nanobodies towards thrombin activatable fibrinolysis inhibitor. *J Thromb Haemost*. 2010;8(6):1302-1312. doi:10.1111/j.1538-7836.2010.03816.x

89. Reverter D, Fernández-Catalán C, Baumgartner R, et al. Structure of a novel leech carboxypeptidase inhibitor determined free in solution and in complex with human carboxypeptidase A2. *Nat Struct Biol*. 2000;7(4):322-328. doi:10.1038/74092

90. Arolas JL, Lorenzo J, Rovira A, Castellà J, Aviles FX, Sommerhoff CP. A carboxypeptidase inhibitor from the tick Rhipicephalus bursa: isolation, cDNA cloning, recombinant expression, and characterization. *J Biol Chem*. 2005;280(5):3441-3448. doi:10.1074/jbc.M411086200

91. Day SM, Reeve JL, Myers DD, Fay WP. Murine thrombosis models. *Thromb Haemost*. 2004;92(9):486-494. doi:10.1055/s-0037-1613739

92. Westrick RJ, Winn ME, Eitzman DT. Murine Models of Vascular Thrombosis. *Arterioscler Thromb Vasc Biol*. 2007;27(10):2079-2093. doi:10.1161/ATVBAHA.107.142810

93. Rosen ED, Raymond S, Zollman A, et al. Laser-Induced Noninvasive Vascular Injury Models in Mice Generate Platelet- and Coagulation-Dependent Thrombi. *Am J Pathol*. 2001;158(5):1613-1622. doi:10.1016/S0002-9440(10)64117-X

94. Benninger RKP, Piston DW. Two-Photon Excitation Microscopy for the Study of Living Cells and Tissues. *Curr Protoc Cell Biol*. 2013;59(1):4.11.1-4.11.24. doi:10.1002/0471143030.cb0411s59

95. Klement P, Liao P, Bajzar L. A Novel Approach to Arterial Thrombolysis. *Blood*. 1999;94(8):2735-2743. doi:10.1182/blood.V94.8.2735.420k30_2735_2743

96. Minnema MC, Friederich PW, Levi M, et al. Enhancement of rabbit jugular vein thrombolysis by neutralization of factor XI. In vivo evidence for a role of factor XI as an anti-fibrinolytic factor. *J Clin Invest*. 1998;101(1):10-14. doi:10.1172/JCI781

97. Nagashima M, Werner M, Wang M, et al. An Inhibitor of Activated Thrombin-Activatable Fibrinolysis Inhibitor Potentiates Tissue-Type Plasminogen Activator-Induced Thrombolysis in a Rabbit Jugular Vein Thrombolysis Model☆. *Thromb Res*. 2000;98(4):333-342. doi:10.1016/S0049-3848(00)00184-5

98. Muto Y, Suzuki K, Sato E, Ishii H. Carboxypeptidase B inhibitors reduce tissue factor-induced renal microthrombi in rats. *Eur J Pharmacol*. 2003;461(2):181-189. doi:10.1016/S0014-2999(03)01297-4